# IMPURITY TRANSPORT IN COLLISIONLESS TRAPPED-PARTICLE-DRIVEN TURBULENCE

M. LESUR
Institut Jean Lamour (IJL), UMR 7198 CNRS / Université de Lorraine
Nancy, France
Email: maxime.lesur@univ-lorraine.fr

E. GRAVIER, K. LIM, C. DJERROUD
Institut Jean Lamour (IJL), UMR 7198 CNRS / Université de Lorraine
Nancy, France

M. IDOUAKASS
National Institute for Fusion Science (NIFS), National Institutes of Natural Sciences (NINS)
Toki, Japan

X. GARBET
CEA, Institut de Recherche sur la Fusion Magnétique (IRFM)
Saint-Paul-lez-Durance, France

**Abstract**

The paper reports on properties of the radial turbulent transport of light to heavy impurities due to trapped-particle-driven turbulence in the core of tokamaks, based on a gyrokinetic bounce-averaged model. The focus is on the effects of impurity concentration, charge, mass, gradients – on impurity transport. The validity of the usual passive treatment of impurities is found to be limited to concentrations of $W^{40+}$ tungsten (respectively, $C^{6+}$ carbon) below $2x10^{-4}$ (1.4%). The diffusive impurity transport decreases slightly with increasing mass number. It depends strongly on the charge number Z, but the effect depends on the nature of turbulence: it increases with Z for turbulence dominated by Trapped Electron Modes (TEM) but decreases with Z for turbulence dominated by Trapped Ion Modes (TIM). The direction of thermo-diffusion also depends on the nature of the turbulence, and on the impurity temperature profile. Finally, the direction of the curvature pinch depends on magnetic shear: it is inward for a positive magnetic shear, while a negative magnetic shear prevents impurity core accumulation, in agreement with quasilinear theory.

## 1. INTRODUCTION

In the context of magnetic confinement fusion plasmas, ion species other than hydrogen isotopes are referred to as impurities. Tokamak plasmas often contain impurities such as helium, tungsten, beryllium, carbon, argon, or neon. Accumulation of impurities in the core threatens the viability of fusion. One issue is the dilution of fuel, which degrades the efficiency of fusion reactors. Another urgent issue is radiative loss, which can be particularly strong for heavy impurities. All in all, the efficiency of fusion is very sensitive to core impurity concentration [1]. Improving theories of impurity transport is crucial to address these urgent issues.

To account for both kinetic and global effects, to which turbulent transport is sensitive, we adopt a global gyrokinetic approach. However, since we base the present exploration on many parameter scans, which would require hundreds of millions of hours of parallel computing if performed with a global 5D gyrokinetic code, we adopt a reduced approach. Namely, we start from a 3D bounce-averaged gyrokinetic model, focusing on particles trapped deeply by the magnetic field inhomogeneity in toroidal geometry. The orbits of these particles live in a 2D phase-space parametrized by an energy invariant.

This approach is meant to explore the basic mechanisms of turbulent transport in collisionless trapped-particle-driven turbulence, rather than to provide quantitative predictions since this in some sense we isolate a part of the complex system of core tokamak turbulence. Here we investigate the impacts of impurity concentration, charge, mass and gradients.

## 2. MODEL

In conventional 5D gyrokinetics, particle motion is described in a 4D phase-space (the 3 coordinates of the gyrocenter + parallel velocity or momentum) parameterized by the gyrokinetic counterpart of the magnetic moment. In contrast, here, we limit the kinetic description to the bounce-averaged dynamics of deeply trapped

particles. Such a particle is parametrized by its precession angle α, its average poloidal magnetic flux $\psi$ (a radial coordinate), and an invariant $E$ akin to a kinetic energy. The distribution function $f_s(\alpha, \psi, E, t)$ of these particles, for each species $s$, is evolved according to a Vlasov equation,

$$\frac{\partial f_s}{\partial t} + [J_0\phi, f_s]_{\alpha,\psi} + \omega_{d,s}\frac{\partial f_s}{\partial \alpha} = 0$$

where $[J_0\phi, f_s]_{\alpha,\psi}$ are Poisson brackets, $J_0$ is a gyrokinetic-gyrobounce operator, $\omega_{d,s}$ is the precession frequency, which depends on both $E$ and the charge number Z.

The other types of particles in the plasma are described via their density response to electric potential fluctuations ϕ, which forms the left-hand-side of the quasineutrality equation,

$$\sum_s \frac{eZ_s^2 n_{eq,s}}{T_{eq,s}}\left[\frac{1-f_t}{f_t}\left(\phi - \epsilon_{\phi,s}\langle\phi\rangle\right) - \bar{\Delta}_s\phi\right] = 4\pi\sqrt{2}\sum_s \frac{Z_s}{m_s^{3/2}}\int_0^\infty J_{0,s} f_s E^{1/2} dE$$

Here $f_t$ is the fraction of trapped particles, $\epsilon_{\phi,s} \in [0,1]$ controls the response of passing particles. Finally, $\bar{\Delta}_s\phi$ is a polarization term, where the Laplacian operator depends on the Larmor radius $\rho_c$ and the banana width $\delta_b$.

The semi-Lagrangian simulation code TERESA has been developed based on this model. The role of kinetic effects was discussed in Refs. [2][3][4]. TERESA was applied in 2018 to a deuterium plasma with non-trace concentrations of tungsten, showing that peaked or hollow impurity density profile can change the nature of turbulence from TEM to TIM [5]. This paper reports on more recent works based on TERESA simulations with a deuterium plasma and various impurities.

## 3. LIMIT OF VALIDITY OF THE PASSIVE TREATMENT

In gyrokinetic simulations, trace impurity species can be either treated self-consistently (what we refer to as active treatment), or, on the contrary, without including them in Maxwell equations (what we refer to as passive treatment). The latter approach is consistent with the assumption that impurities with low enough concentrations are impacted by turbulence generated by electrons and main ions, but do not impact it significantly in return. Indeed, the relative contribution of impurity density in quasi-neutrality is of the order of $C.Z^2$, where C is the impurity concentration, and Z its charge number. In the "trace" limit ($C.Z^2 << 1$), the impurity behaves as a passive species, or test-particle, which means that its presence does not affect the turbulent state.

In this section, which is based on Ref. [6], we relax this assumption, and investigate the impacts of impurity, on impurity transport, as a function of its concentration, in the presence of trapped-particle-driven turbulence. We run a series of simulations with self-consistent (active) treatment of impurities for a wide range of concentrations and compare the results with a series of simulations with passive treatment of impurities.

### 3.1. Impact of tungsten concentration

For each species, the equilibrium distribution function is chosen as 2D Maxwellian with radial density profile such that $\kappa_n = |dn/d\psi|$ =const. and similarly for the temperature profile with gradient $\kappa_T$. The impacts of tungsten concentration depend on the relationship between equilibrium density gradient and temperature gradient [6]. Here we focus on a case where these gradients are equal. The gradients and the simulation parameters are given in Table 1. Thermal baths are imposed at both radial boundaries.

TABLE 1. SIMULATION PARAMETERS

| $a/R_0$ | $f_t$ | $\kappa_n = \kappa_T$ |
|---|---|---|
| 0.1 | 2/3 | 0.25 |

| Species | Z | $\rho_c/a$ | $\delta_b/a$ | $\epsilon_{\phi,s}$ | Concentration | $T_e/T_i$ |
|---|---|---|---|---|---|---|
| Electrons | -1 | 0.01 | 0.01 | 1 | 1 | 1 |
| Deuterium | 1 | 0.03 | 0.1 | 0 | 1 – 40 C | 1 |
| Tungsten | 40 | 0.0072 | 0.024 | 0 | C | 1 |

*FIG. 1* summarizes the impact of $W^{40+}$ concentration. It includes the relative variation, due to the presence of impurity, of linear growth rate, turbulence intensity, and impurity density flux. For example, the relative variation of linear growth rate is $(\gamma - \gamma_0)/\gamma_0$, where $\gamma_0$ is the growth rate when C=0. A similar definition is used for turbulence intensity. As for the impurity density flux, it is normalised to C, and the variation is with respect to the impurity flux in the trace limit. We note $\omega_0$ the precession frequency of particles with velocity equal to the Deuterium thermal speed. The measured impact of impurity concentration on linear growth rate $\gamma$ for $C<10^{-3}$ agrees with the analytic expression $\gamma = \gamma_0 - C\, d\gamma$ with $d\gamma = 2.2 \times 10^{-4}\omega_0$, which was obtained at first order in C in the appendix 1 of Ref. [6]. The stabilizing effect of impurity on TEM is consistent with Refs. [7][8], although our interpretation differs: we have shown that this is mainly due to a modification of the response of passing particles when $C.Z^2 \sim 1$. The measured impact of impurity concentration on turbulence intensity is in qualitative agreement with a mixing length estimate, $e\phi/T_0 = \gamma/(k_r \rho_{c,i} k_\theta c_s)$. However, the rms of the potential is twice more sensitive to C than predicted from the latter estimate.

Furthermore, the sensitivity of impurity density flux to C is even more threshold-like than expected from the sensitivity of turbulence intensity. As observed on *FIG. 1*, there is a transition for all linear growth rate, turbulence intensity, and impurity density and heat fluxes, centred around $C.Z^2 = 1.1$. However, the transition is significantly steeper for the fluxes. This transition may be viewed as a threshold, which gives the range of validity of the passive treatment, $C < 2.10^{-4}$. When the temperature gradient is finite and the density profile is flat, we obtain qualitatively similar results, except for the density flux which vanishes. For the heat flux, the range of validity of the passive treatment is slightly smaller than for the case with equal gradients, $C < 10^{-4}$.

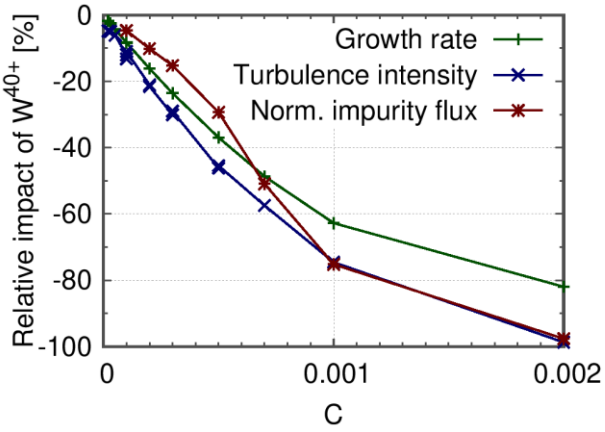


*FIG. 1. Relative variation, due to the presence of impurity, of linear growth-rate, turbulence intensity (rms of the potential), and density flux, all versus tungsten concentration C. Here the impurity flux is normalised to the impurity density, and the variation is relative to the trace limit.*

### 3.2. Impact of carbon concentration

We have performed a similar analysis for $C^{6+}$ carbon. There are two qualitative differences compared with the tungsten case:

— The transition for the flux is centred around $C.Z^2 = 0.5$;
— The transition for the flux is at lower concentration than the transition for turbulence intensity and growth-rate, which is opposite to the tungsten case.

However, our main conclusion stands: the transition is steeper for the flux than for turbulence, and steeper for turbulence than for the growth-rate.

### 3.3. Synchronisation between impurity density and electric potential fluctuations

We have investigated the physical mechanism responsible for this difference in behaviour between turbulence intensity and transport. We observe that phase-synchronization between impurity density fluctuations and electric potential fluctuations occurs for high enough impurity concentrations, which quenches impurity transport.

## 4. DIFFUSIVE TRANSPORT, THERMO-DIFFUSIVE PINCH, AND CURVATURE-DRIVEN PINCH

Hereafter, the impurity species are treated self-consistently but in the trace limit, so that impurity concentrations do not affect the nature of the turbulence.

### 4.1. Impact of charge and mass numbers on diffusion

To evaluate impurity transport, we plot the cumulative flux along the $\psi$-direction (meaning along the radial direction) given by

$$\Gamma_{\text{cumul}} = \int_0^t \Gamma(t^*)\mathrm{d}t^*$$

with

$$\Gamma(t) = -\frac{2}{\sqrt{\pi}}\int_0^{2\pi} d\alpha \int_0^{\infty} f \frac{\partial(\mathcal{J}\phi)}{\partial\alpha} E^{1/2}\,\mathrm{dE}$$

The impurity flux due to Trapped Electron Mode (TEM) turbulence increases with (A,Z) (*FIG. 2*). In contrast, the impurity flux is found to decrease with (A,Z) when the Trapped Ion Mode (TIM) dominated (*FIG. 3*). In this case the higher charge impurity has smaller impurity flux. In fact, we have shown [9] that the dependency on mass number A is much weaker than the dependency on the charge number Z.

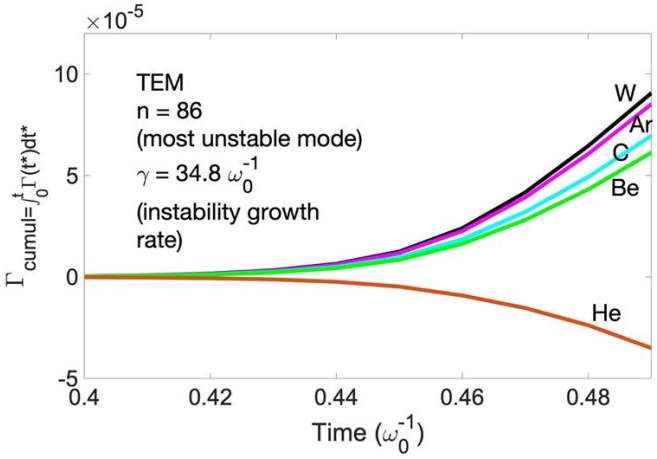


*FIG. 2. Impurity cumulative flux plotted against time in the case of a TEM turbulence. Helium diffuses from the core to the edge while other impurities diffuse from the edge to the core, according to the initial density gradients.*

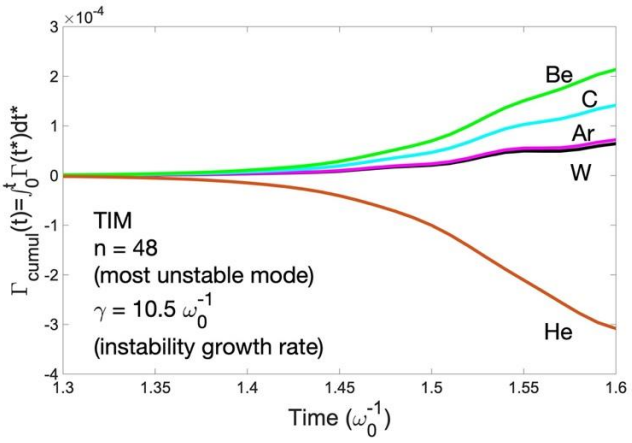


*FIG. 3. Impurity cumulative flux plotted against time in the case of a TIM turbulence. Helium diffuses from the core to the edge while other impurities diffuse from the edge to the core, according to the initial density gradients.*

Let us compare the theoretically predicted impurity flux and the nonlinear impurity transport simulations. Quasi-linear theory yields:

$$\frac{\partial n_0}{\partial t} + \frac{\partial \Gamma_\psi}{\partial \psi} = 0$$

with $\Gamma_\psi$ the impurity transport in the radial direction:

$$\Gamma_\psi = -\kappa_n \int_E \sum_n |n\mathcal{J}\phi_n|^2 \frac{\gamma_n}{\left(\omega_{r,n} - n\frac{\Omega_d}{Z}E\right)^2 + \gamma_n^2} F_{eq_{\psi=0}} E^{1/2} dE$$

Both $\gamma_n$ and $\omega_{r,n}$ have very weak dependency on both $Z$ and $A$, since only trace impurities are considered, and therefore turbulence is governed by electrons and main ions. Therefore, from this last equation we can see that the radial impurity flux depends on the charge number $Z$ as expected but depends weakly on the mass number. Indeed, the impurity mass only impacts the gyro-bounce-averaging operator, where the Larmor radius and the banana width are proportional to $\sqrt{A}/Z$. But this $A$-dependence of the gyro-bounce-averaging operator is weak and does not depend on the sign of $\omega_r$ and the nature of the instability. Nevertheless, regarding the $A$-dependence, the impurity flux is expected to decrease as $A$ increases, in both TEM and TIM cases. These results agree with the numerical simulations.

This expression can be further evaluated by considering two different cases: negative and positive frequencies. The real frequencies $\omega_{r,n}$ and the linear growth rates $\gamma_n$ are needed and determined by solving the linear dispersion relation. The saturation level of the plasma potential is given by nonlinear simulations.

Here, we choose five different impurities with the same mass number (A = 20) but with 5 different charge numbers Z = 2, 4, 8, 10 and 12. We describe how impurity diffusive transport depends on the charge number, depending on the nature of the dominant instabilities: the diffusion coefficient increases with Z in the case of TEM turbulence [9] (*FIG. 4*), while it decreases with Z in TIM-dominated turbulence, in good agreement with quasilinear theory.

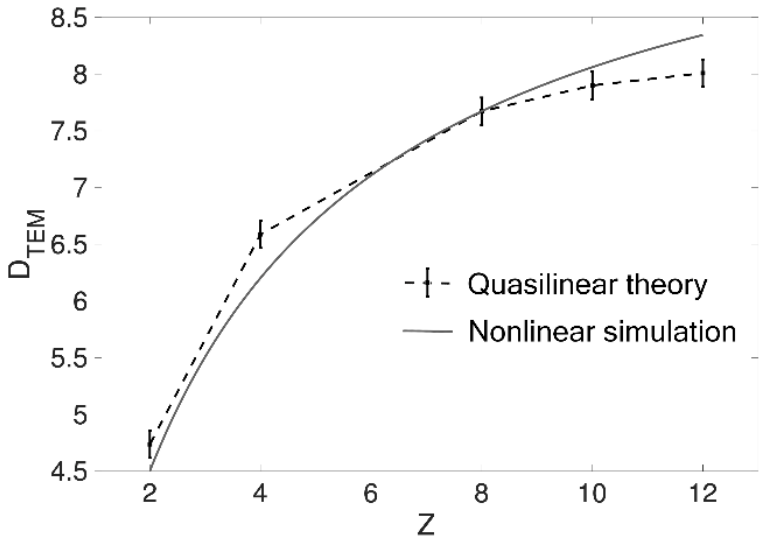


*FIG. 4. Impurity diffusion coefficient $D_{TEM}$ plotted against the impurity charge number Z in the case of TEM turbulence.*

### 4.2. Thermo-diffusive pinch in TIM and TEM turbulences

The total particle flux – consisting of the diffusive and convective part – can be decomposed into

$$\frac{\Gamma_z}{N_z} = -D_z \frac{\nabla N_z}{N_z} + V_z = \underbrace{+D_z \kappa_{nz}}_{Diffusion} + \underbrace{V_z}_{Convection}$$

with

$$V_z \propto C_T \kappa_{Tz} + C_P$$

The first term in the pinch velocity $V_z$ corresponds to the thermo-diffusive pinch which stems from the inherent temperature gradient while the second term is the curvature pinch, proportional to magnetic field curvature.

Here, we use five different values of impurity temperature profiles to investigate the thermo-diffusive pinch with no magnetic curvature ($C_P = 0$). *FIG. 5* shows that, as expected, the pinch velocity $V_z$ disappears when the temperature profile is flat. $V_z$ changes its sign when the temperature gradient does. We observe that the sign of the coefficient $C_T$ changes depending on the TIM or TEM nature of the turbulence at a given temperature gradient [10]. Here, $\kappa_{Tz} > 0$ means that the core is hotter than the edge, therefore the right part of the figure is more relevant. In this case, curvature pinch is inward except for reversed magnetic shear, consistently with [11].

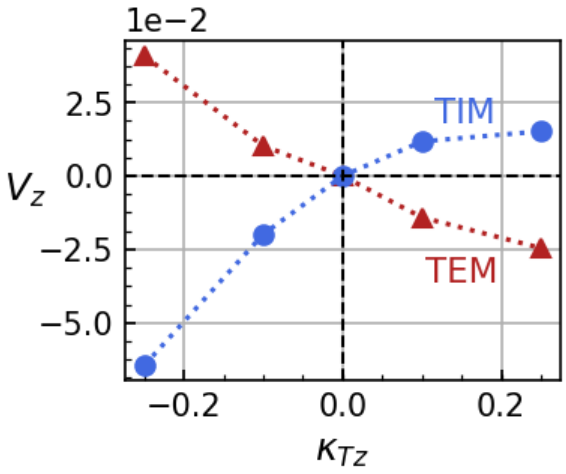


*FIG. 5. Thermodiffusion velocity $V_Z$ plotted against the impurity temperature gradient, for both TEM and TIM turbulences.*

### 4.3. Impact of magnetic shear on curvature pinch

In a similar way that thermo-diffusive pinch was studied by imposing $C_P = 0$, the direction of magnetic curvature pinch can be investigated by imposing a flat temperature gradient for the impurity ($\kappa_{Tz} = 0$). Given that the Maxwellian distribution function $F_{eq}$ contains the effect of magnetic curvature through the Hamiltonian $H_{eq} = \frac{1}{2} m {v_\parallel}^2 + \mu B$, the manipulation of magnetic curvature can be readily achieved by changing $H_{eq}$.

$$F_{eq} = \frac{N_{eq}}{T_{eq}^{3/2}} \exp\left(-\frac{H_{eq}}{T_{eq}}\right)$$

In the bounce-averaged gyrokinetic code, the Hamiltonian can be expressed in terms of toroidal precession frequency $\Omega_d$ which is a characteristic frequency of trapped particles.

$$H_{eq} = E(1 + e\alpha\Omega_d\psi)$$

where α is an ad-hoc coefficient which determines the positive/negative magnetic shear according to its sign.

A positive value of α represents a positive magnetic shear while a negative value of α mimics a negative magnetic shear. The direction of the curvature pinch $V_Z$ with different values of α is represented in *FIG. 6*. Our simulations show that the direction of the impurity curvature pinch is inward in the case of a positive magnetic shear, while a negative magnetic shear switches the sign of $V_Z$ and therefore prevents impurity core accumulation. This is in qualitative agreement with quasilinear theory.

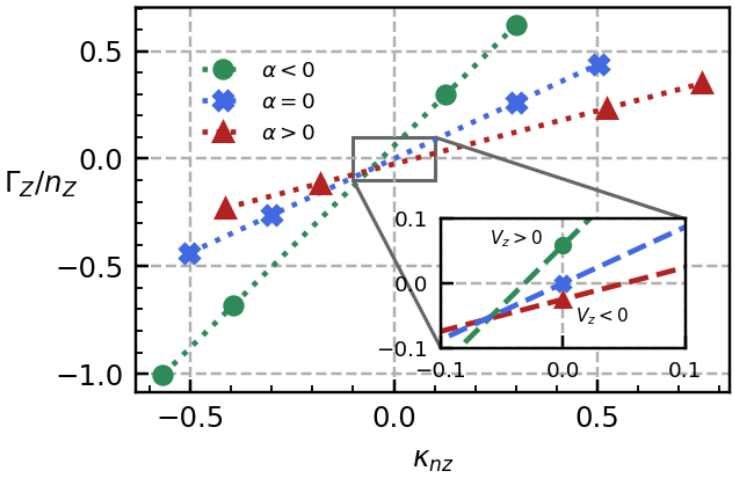


*FIG. 6. Magnetic curvature pinch $V_Z$ plotted with different values of α (with flat temperature gradient of impurity). The sign of α is representative of the sign of magnetic shear*.

## 5. SUMMARY, CAVEATS AND PERSPECTIVES

To summarize, we first analysed the impact of impurity concentration on mode growth, saturation amplitude, and transport in TEM/TIM turbulence. There is a transition for all growth rate, turbulence intensity, and impurity density and heat fluxes, centered around $C.Z^2 = 1.1$ for $W^{40+}$ and 0.5 for $C^{6+}$. However, the transition is significantly steeper for the fluxes due to phase-synchronization between electric potential fluctuations and impurity density fluctuations for high enough concentrations. The range of validity of the passive treatment of tungsten is limited to concentrations smaller than $10^{-4}$ (in order of magnitude).

Secondly, the nonlinear simulations demonstrate that, in qualitative agreement with quasi-linear theory :

— Impurity diffusive transport decreases (increases) with Z in TIM (TEM) turbulence. The dependency on mass number is much weaker;
— For standard impurity temperature gradient, thermo-diffusion brings impurities outwards (inwards) in TIM (TEM) turbulence.
— Curvature pinch is inward except for reversed magnetic shear.

The model used in the above analyses is collisionless and limited to trapped-particle-driven turbulence. We applied it as a prototype of turbulent transport in toroidal fusion plasmas to draw qualitative trends. Although this is outside the scope of this paper, we have recently made progress using more advanced models. Firstly, ITG modes must be included for the quasi-steady-state turbulent spectrum to be more accurate. Secondly, in general, both collisional (neoclassical) and turbulent processes contribute to the radial transport of impurities, in some conditions in synergy [12][13][14]. It turns out that an accurate collision operator is crucial. Thirdly, sources and boundary conditions can have significant impacts. The new version of the GYSELA-X gyrokinetic code is well-adapted in these respects. Recently we have been applying it to investigate impurity transport [15].

## ACKNOWLEDGEMENTS

This work was carried out within the framework of the French Federation for Magnetic Fusion Studies (FR-FCM) and of the EUROfusion Consortium. It received funding from the Agence Nationale de la Recherche for the project GRANUL (ANR-19-CE30-0005), and from the Euratom research and training programmes 2014-2018 and 2019-2020 under Grant Agreement No. 633053 for the project WP17-ENRCEA-02. The views and opinions expressed herein do not necessarily reflect those of the European Commission. This work was granted access to the HPC resources of IDRIS under allocations 2019 and 2020 made by GENCI, of EXPLOR under Project No. 2017M4XXX0251, and of CINECA Marconi under projects GSNTIT and GSNTITS.

## REFERENCES

[1] PÜTTERICH, T., NEU, R., DUX, R., WHITEFORD, A.D., O'MULLANE, M.G., SUMMERS, H.P., Calculation and experimental test of the cooling factor of tungsten, Nucl. Fusion **50** (2010) 025012.

[2] LESUR, M., CARTIER-MICHAUD, T., DROUOT, T., DIAMOND, P.H., KOSUGA, Y., REVEILLE, T., GRAVIER, E., GARBET, X., ITOH, S.I., ITOH, K., A simple model for electron dissipation in trapped ion turbulence, Phys. Plasmas **24** (2017) 012511.

[3] MEDINA, J., LESUR, M., GRAVIER, E., REVEILLE, T., IDOUAKASS, M., DROUOT, T., BERTRAND, P., CARTIER-MICHAUD, T., GARBET, X., DIAMOND, P.H., Radial density and heat fluxes description in the velocity space: nonlinear simulations and quasi-linear calculations, Phys. Plasmas **25** (2018) 122304.

[4] MEDINA, J., LESUR, M., GRAVIER, E., REVEILLE, T., BERTRAND, P., Test particle dynamics in low-frequency tokamak turbulence, Phys. Plasmas 26 (2019) 102301.

[5] IDOUAKASS, M., GRAVIER, E., LESUR, M., MEDINA, J., REVEILLE, T., DROUOT, T., GARBET, X., SARAZIN, Y., Impurity density gradient influence on trapped particle modes, Phys. Plasmas **25** (2018) 062307.

[6] LESUR, M., DJERROUD, C., LIM, K., GRAVIER, E., IDOUAKASS, M., MORITZ, J., MEDINA, J., REVEILLE, T., DROUOT, T., CARTIER-MICHAUD, T., Validity limits of the passive treatment of impurities in gyrokinetic tokamak simulations, Nucl. Fusion **60** (2020) 036016.

[7] DU, H., WANG, Z.X., DONG, J.Q., LIU, S.F., Coupling of ion temperature gradient and trapped electron modes in the presence of impurities in tokamak plasmas, Phys. Plasmas **21** (2014) 052101.

[8] DU, H., WANG, Z.X., DONG, J.Q., Impurity effects on trapped electron mode in tokamak plasmas, Phys. Plasmas **23** (2016) 072106.

[9] GRAVIER, E., LESUR, M., GARBET, X., SARAZIN, Y., MEDINA, J., LIM, K., IDOUAKASS, M., Diffusive impurity transport driven by trapped particle turbulence in tokamak plasmas, Phys. Plasmas **26** (2019) 082306.

[10] LIM, K., GRAVIER, E., LESUR, M., GARBET, X., SARAZIN, Y., MEDINA, J., Impurity pinch generated by trapped particle driven turbulence, Plasma Phys. Control. Fusion **62** (2020) 095018.

[11] FUTATANI, S., GARBET, X., BENKADDA, S., DUBUIT, N., Reversal of impurity pinch velocity in tokamaks plasma with a reversed magnetic shear configuration, Phys. Rev. Lett. **104** (2010) 015003.

[12] ESTEVE, D., SARAZIN, Y., GARBET, X., GRANDGIRARD, V., BRETON, S., DONNEL, P., ASAHI, Y., BOURDELLE, C., DIF-PRADALIER, G., EHRLACHER, C., Self-consistent gyrokinetic modeling of neoclassical and turbulent impurity transport, Nucl. Fusion **58** (2018) 036013.

[13] ASAHI, Y., GRANDGIRARD, V., SARAZIN, Y., DONNEL, P., GARBET, X., IDOMURA, Y., DIF-PRADALIER, G., LATU, G., Synergy of turbulent and neoclassical transport through poloidal convective cells, Plasma Phys. Control. Fusion **61** (2019) 065015.

[14] IDOMURA,Y., OBREJAN, K., ASAHI, Y., HONDA, M., Dynamics of enhanced neoclassical particle transport of tracer impurity ions in ion temperature gradient driven turbulence, Phys. Plasmas **28** (2021) 012501.

[15] LIM, K., GARBET, X., SARAZIN, Y., GRANDGIRARD, V., OBREJAN, K., LESUR, M., GRAVIER, E., Gyrokinetic modelling of light to heavy impurity transport in tokamaks, Nucl. Fusion **61** (2021) 046037.